Supporting Information For: Understanding the Plasmon Resonance in Ensembles of Degenerately Doped Semiconductor Nanocrystals

Rueben J. Mendelsberg,[†,§] Guillermo Garcia,[†] Hongbo Li,[‡] Liberato Manna,[‡] and Delia J. Milliron[*,¶]

Lawrence Berkeley National Laboratory, The Molecular Foundry, Berkeley California, 94720 , Istituto Italiano di Tecnologia, Via Morego 30, 16163 Genova, Italy , and Lawrence Berkeley National Laboratory, Molecular Foundry, Berkeley California, 94720

E-mail: dmilliron@lbl.gov

Comparing Mie and MG-EMA Results

In order to explore the similarity and difference between the absorbance calculated by the Mie theory (A_{Mie}) and the Maxwell-Garnett (MG) effective medium approximation (A_{MG}), both were calculated using the Drude dielectric function for a range of volume fractions f_{V} and bulk plasma frequencies (ω_{P}). For each case, the optical path length L was adjusted such that $f_{\mathrm{V}} * L$ was kept constant. In this way, the total volume of the absorbing material is kept constant, resulting in comparable absorbance values for all f_{V}. The mean-square-difference (MSD) between A_{Mie} and A_{MG} is shown in Fig. S1.

[*]To whom correspondence should be addressed
[†]Lawrence Berkeley National Laboratory, The Molecular Foundry, Berkeley California, 94720
[‡]Istituto Italiano di Tecnologia, Via Morego 30, 16163 Genova, Italy
[¶]Lawrence Berkeley National Laboratory, Molecular Foundry, Berkeley California, 94720
[§]Lawrence Berkeley National Laboratory, Plasma Applications Group, Berkeley California, 94720
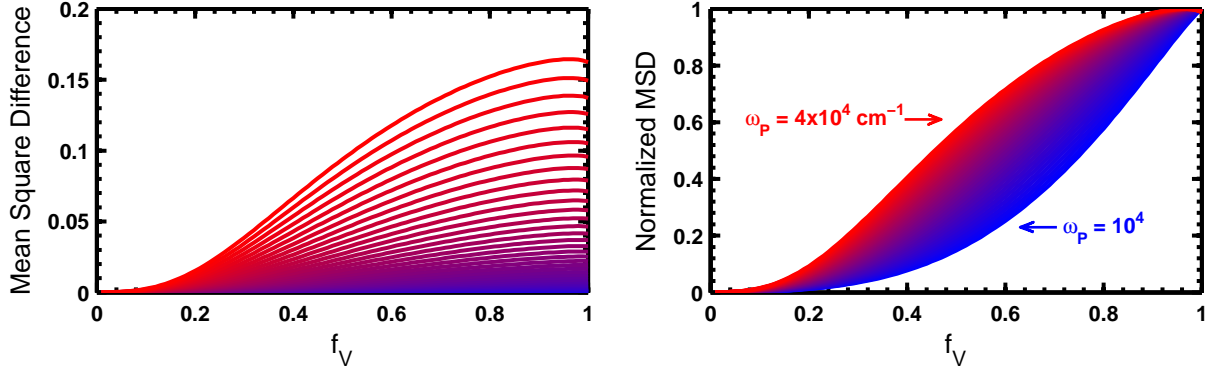
1

Figure S1: Mean square difference (MSD) between absorbance calculated by Mie theory and effective medium theory for a range of plasma frequencies (ω_P). Absolute value on the left and normalized to the maximum value on the right.

At a constant f_V, the absorbance naturally increases as ω_P increases. Thus, the magnitude of the MSD between A_{Mie} and A_{MG} will also increase. Fig. S1(b) shows the normalized MSD and indicates a slight difference in the shape of the curve depending on ω_P. Nevertheless, for all ω_P in the range of 10,000 to $40,000\,\mathrm{cm}^{-1}$, A_{Mie} and A_{MG} are essentially identical when $f_V < 0.1$.
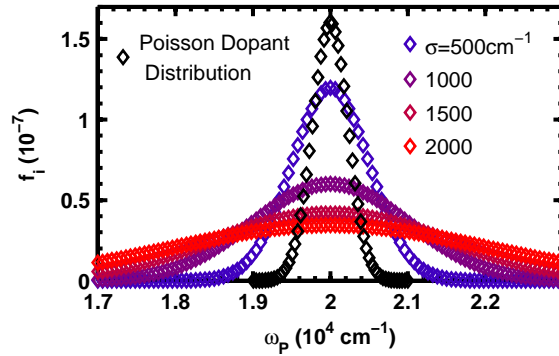
Dopant Inhomogeneity

Figure S2: Discrete distributions of plasma frequencies used when exploring dopant concentration inhomogeneity within an ensemble of nanocrystals. In each case $\sum f_i = f_V = 2.5 \times 10^{-5}$. The black dots are the approximate distribution of ω_P for an ideal ensemble showing a Poisson distribution of dopants.

Fig. S2 shows some examples of the Gaussian plasma frequency distributions used to explore

the effect of dopant inhomogeneity. In the ideal case, the dopants will be distributed according to Poisson statistics.[1] The distribution shown in Fig. S2 labeled "Poisson" was calculated for $4.5\,\text{nm}$ indium-tin-oxide (ITO) nanocrystals with $14\,\text{at\%}$ Sn, of which 16.5% contributes free-carriers. This gives a mean plasma frequency of $20,000\,\text{cm}^{-1}$, in-line with the rest of the calculations. The Poisson distribution of dopants translates into a nearly Gaussian shape in the distribution of ω_P with a standard deviation of about $\sigma = 250\,\text{cm}^{-1}$.
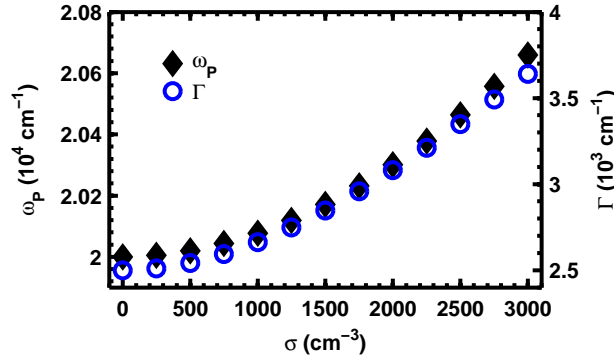

Figure S3: Values extracted from an inhomogeneously doped ensemble when assuming the ensemble is homogeneous with a single plasma frequency.

If the absorbance from an inhomogeneously doped ensemble is fit with a model assuming all nanocrystals are identical, the extracted ω_P and Γ are in error as shown in Figure S3.

Size Dependence of Γ

The size dependence of the plasmon damping, Γ, was calculated using $\Gamma(R) = \Gamma_0 + Cv_F/R$ where Γ_0 is the bulk damping constant, v_F is the Fermi velocity and C is a theory dependent constant.[2] In order to get values which are consistent with Γ extracted from previous work on ITO nanocrystals,[3,4] the constants used for the calculation were $\Gamma_0 = 1000\,\text{cm}^{-1}$, $v_F = 1 \times 10^8\,\text{cm/s}$,[5] and $C \approx 0.1$ which results in the curve shown in Figure S4.

Γ_0 and v_F are near the accepted values but C is significantly less than that typically used for metals ($C = 1$).[2] However, using $C = 0.1$ gives $\gamma = 2,500\,\text{cm}^{-1}$ for nanocrystals with a mean
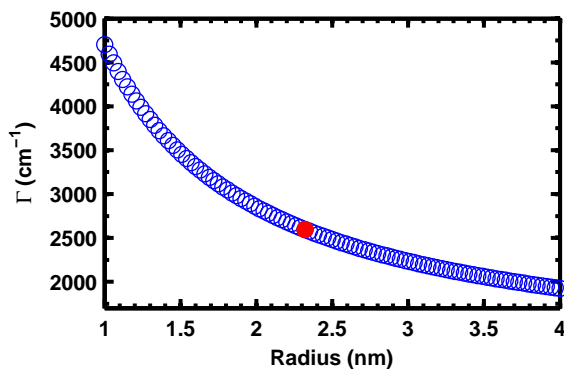
Figure S4: Γ as a function of particle radius (R) used to convert the log-normal size distribution into a Γ-distribution. The solid red dot shows the most probable R used in the subsequent calculations.

radius of $\approx 5\,\text{nm}$. This serves as a good approximation to the ITO nanocrystals used in this work and so the curve in Figure S4 gives a realistic approximation of $\Gamma(R)$. Furthermore, the end results do not change by much if the most probable R lies on a steeper or shallower part of the $\Gamma(R)$ curve.

Colloidal chemistry techniques can create relatively narrow size distributions of many compounds. Example size distributions measured from about 100 particles for ITO and $Cu_{1.85}Se$ nanocrystals is shown in Figure S5 along with the best fit of a log-normal distribution.[6] Despite only counting 100 particles, it is clear that the half width at half maximum is about 15% for these particles.
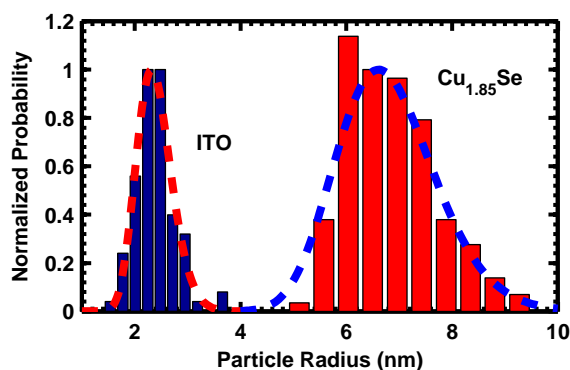

Figure S 5: Measured distribution of particle radius in ensembles of In_2O_3:Sn and $Cu_{1.85}Se$ nanocrystals by TEM image analysis with about 100 particles counted in each case. The dotted lines show fits of a log-normal distribution.

Core-Shell Effective Medium Approximation

Using the core-shell EMA discussed in the main text, absorbance of Drude nanocrystals with a ligand shell ($\varepsilon_s = 2.13$) dispersed in a host of air ($\varepsilon_H = 1$) can be calculated as shown in Figure S6. Depending on the shell thickness, the resulting peak position is in between that expected for shell-free particles in the actual host and shell-free particles in a host with the same dielectric constant as the shell.
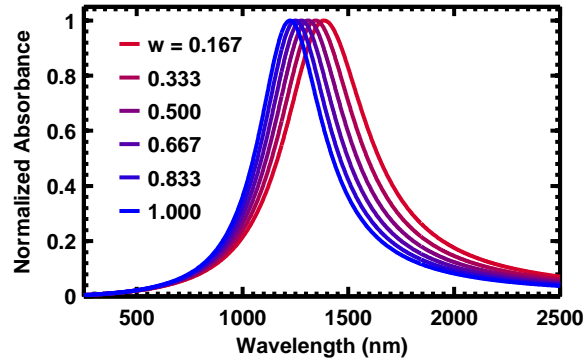

Figure S 6: Calculated absorbance of Drude nanocrystals with a ligand shell with $\varepsilon_s = 2.13$ at various core volume fractions (w) in a host of air to exaggerate the screening effect of the shell.

Error in Simple LSPR Frequency Approximation

As discussed in the main text, the common approximation for the expected LSPR frequency contains inherit error. Also discussed was that this error depends on ω_P and ε_H. Here the dependence of the error on ε_∞ is shown in Figure S7. Materials with large ε_∞ show the most deviation from the simple approximation for a given plasma frequency.
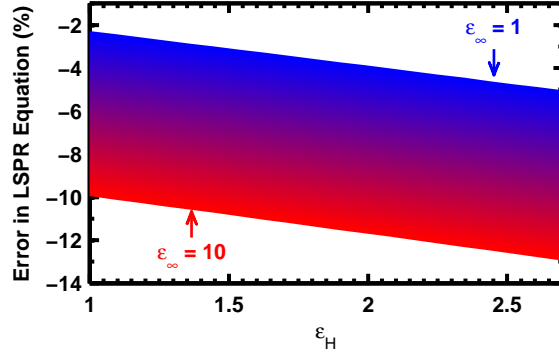
Figure S7: Relative error in the LSPR equation for $\omega_P = 20{,}000\,\mathrm{cm}^{-1}$ as a function of ε_H and ε_∞

Real Dispersions

Materials

Dispersions of $Cu_{2-x}Se$ and ITO in TCE were prepared by colloidal chemisty techniques described in previous work.[3,7,8] The samples used in this study were about $13.5\,\mathrm{nm}$ and $4.5\,\mathrm{nm}$ in diameter for the $Cu_{1.85}Se$ and ITO respectively. The ITO contained about $14\,\mathrm{at\%}$ Sn as measured by inductively coupled plasma optical emission spectroscopy (ICP-OES) and it was the exact same batch of nanocrystals used in a previous report that contains further TEM images and XRD spectra of these nanocrystals.[4] ICP-OES also showed $x \approx 0.15$ for the $Cu_{2-x}Se$ used in this study.

Ionized Impurity Scattering

In oxide semiconductors like doped ZnO and ITO, it is well known that ionized impurity scattering must be accounted for when modeling the transmittance and/or absorbance.[4,9,10] This scattering mechanism gives a frequency dependence to the Drude damping constant, which can be described using an empirical formula[4,11]

$$\Gamma(\omega) = \Gamma_L - \frac{\Gamma_L - \Gamma_H}{\pi}\left[\arctan\left(\frac{\omega - \Gamma_X}{\Gamma_W}\right) + \frac{\pi}{2}\right] \tag{1}$$

where Γ_L is the low frequency damping constant, Γ_H is the high frequency damping constant, Γ_X is the cross-over frequency and Γ_W is the cross-over width. This function successfully accounts for the observed asymmetry in the absorbance of the ITO dispersion. For chalcogenides like $Cu_{2-x}Se$ and other materials with a high ε_∞, the absorbance peak is symmetric since the ionized impurities are effectively screened from the free carriers. Thus, assuming a frequency independent Γ is appropriate for those materials.

References

(1) Bryan, J. D.; Gamelin, D. R. *Prog. Inorganic Chem.* **2005**, *54*, 47–126.

(2) Ghosh, S. K.; Pal, T. *Chem. Rev.* **2007**, *107*, 4797–4862.

(3) Garcia, G.; Buonsanti, R.; Runnerstrom, E. L.; Mendelsberg, R. J.; Llordes, A.; Anders, A.; Richardson, T. J.; Milliron, D. J. *Nano Lett.* **2011**, *11*, 4415–4420.

(4) Mendelsberg, R. J.; Garcia, G.; Milliron, D. J. *J. Appl. Phys.* **2012**, *111*, 063515.

(5) Chiu, S.-P.; Chung, H.-F.; Lin, Y.-H.; Kai, J.-J.; Chen, F.-R.; Lin, J.-J. *Nanotechnology* **2009**, *20*, 105203.

(6) Dushkin, C. D.; Saita, S.; Yoshie, K.; Yamaguchi, Y. *Adv. Colloid Interface Sci.* **2000**, *88*, 37–78.

(7) Dorfs, D.; Hartling, T.; Miszta, K.; Bigall, N. C.; Kim, M. R.; Genovese, A.; Falqui, A.; Povia, M.; Manna, L. *J. Am. Chem. Soc.* **2011**, *133*, 11175–11180.

(8) Scotognella, F.; Della Valle, G.; Srimath Kandada, A. R.; Dorfs, D.; Zavelani-Rossi, M.; Conforti, M.; Miszta, K.; Comin, A.; Korobchevskaya, K.; Lanzani, G.; Manna, L.; Tassone, F. *Nano Lett.* **2011**, *11*, 4711–4717.

(9) Hamberg, I.; Granqvist, C. G. *J. Appl. Phys.* **1986**, *60*, R123–R159.

(10) Pflug, A.; Sittinger, V.; Ruske, F.; Szyszka, B.; Dittmar, G. *Thin Solid Films* **2004**, *455-456*, 201–206.

(11) Mergel, D.; Qiao, Z. *J. Phys. D* **2002**, *35*, 794–801.